ONLINE SUPPLEMENT

Shared and distinct rupture discriminants of small and large intracranial aneurysms

Supplemental Methods

Clinical Data Collection

We collected clinical information that we determined to be relevant to intracranial aneurysm (IA) rupture from medical records available at the time of imaging. Patient characteristics included sex, hypertension (HTN; systolic blood pressure >140 mmHg), smoking habits (historical or current), family history of IA, previous subarachnoid hemorrhage (SAH), coronary artery disease, dyslipidemia, diabetes, cocaine use, and polycystic kidney disease.

We also considered aneurysm characteristics, including the presence of multiple IAs and aneurysm location. Aneurysm locations were classified as anterior cerebral artery (ACA, including anterior communicating artery aneurysms), internal carotid artery (ICA, including ophthalmic and superior hypophyseal artery aneurysms), middle cerebral artery (MCA), posterior communicating artery (PCOM, including anterior choroidal artery aneurysms), or posterior circulation (including vertebral, posterior inferior cerebellar, posterior cerebral, superior cerebellar, anterior inferior cerebellar, and basilar artery aneurysms).

Building the Aneurysm Computational Models

IAs were assessed for morphologic and hemodynamic features by segmenting and reconstructing 3D images of the IAs and surrounding vasculature from digital subtraction angiography or computed tomography images. Segmentation was accomplished using the open-source software Vascular Modeling Toolkit (http://www.vmtk.org),[1] and a surface mesh was generated using the threshold-based marching cubes algorithm.[2]

IA computational models were cleaned and volumetrically meshed using ANSYS ICEM Computational Fluid Dynamics (CFD) software (ANSYS Inc., Canonsburg, PA). The proximal ends of the models were confirmed to be 10 diameters from the IA to ensure fully developed flow, and the distal ends were terminated at the next bifurcation. The volumetric mesh consisted of tetrahedral elements with 4 prism layers at the wall to ensure convergence of wall hemodynamic parameters. In our entire IA database, each geometries had between 300,000 and 1,500,000 elements.

Analysis of Aneurysm Morphologic Features

We analyzed morphologic features of each IA from the 3D surface reconstructions. The parameters are described in detail elsewhere and in Supplemental Table 1.[3-5] Briefly, ***IA size*** is the maximum perpendicular height of the aneurysm. ***Neck diameter*** is the average length of the neck plane. ***Size ratio*** (SR) is the relationship between IA size and parent vessel size. ***Aspect ratio*** (AR) is the relationship between IA size and neck diameter. ***Undulation index*** (UI) is the degree of surface irregularity. ***Ellipticity index*** (EI) is an IA's deviation from a perfect hemisphere. ***Nonsphericity index*** (NSI) is an IA's deviation from a perfect hemisphere including surface undulations. Finally, the ***Aneurysm number*** (*An*) is a dimensionless parameter describing the formation of a vortex across the IA neck plane.

Analysis of Aneurysm Hemodynamic Features

We analyzed hemodynamic features associated with IA rupture by CFD. As previously described,[6] a pulsatile waveform measured from transcranial Doppler ultrasound obtained from a healthy volunteer was applied at the inlet boundary. The mean velocity was scaled based on the inlet diameter. A flow split boundary condition was imposed at the outlet boundaries,[7] and a no-slip boundary condition was applied to the walls. Blood was assumed to be incompressible and Newtonian with a density of 1056 kg/m^3 and a viscosity of 0.0035 Ns/m^2. The transient Navier-

Stokes equations were solved at a time step of 0.001 seconds. A pressure implicit splitting of operators (PISO) algorithm was used for temporal discretization, and a first-order upwind differencing scheme was used for spatial discretization. The simulations were run for 3 cycles to ensure convergence of the solution, and the last (third) cycle was used for analysis. Computational simulations were performed using STAR-CCM+ (CD-Adapco, Melville, NY).

Details of the calculation of hemodynamic parameters analyzed in this study can be found in previous publications and in Supplemental Table I.[6, 8] Briefly, ***wall shear stress*** (WSS) is the tangential or friction force on the vessel wall. ***Maximum WSS*** (MWSS) is the maximum intra-aneurysmal WSS. The ***low wall shear stress area*** (LSA) is the surface area of the aneurysm that experiences low WSS (<10% of parent vessel WSS), normalized by the total aneurysm surface area. ***WSS gradient*** (WSSG) is the change in WSS magnitude direction. ***Oscillatory shear index*** (OSI) is the directional change in WSS throughout the cardiac cycle. ***Relative residence time*** (RRT) reflects the relative time of blood at the wall. ***Energy loss*** (EL) is the energy expenditure due to viscous friction, and the ***pressure loss coefficient*** (PLc) is the pressure loss due to geometric irregularities and energy expenditure. Post-processing was performed using Tecplot 360 (Tecplot Inc., Bellevue, WA).

Supplemental Figure and Figure Legend

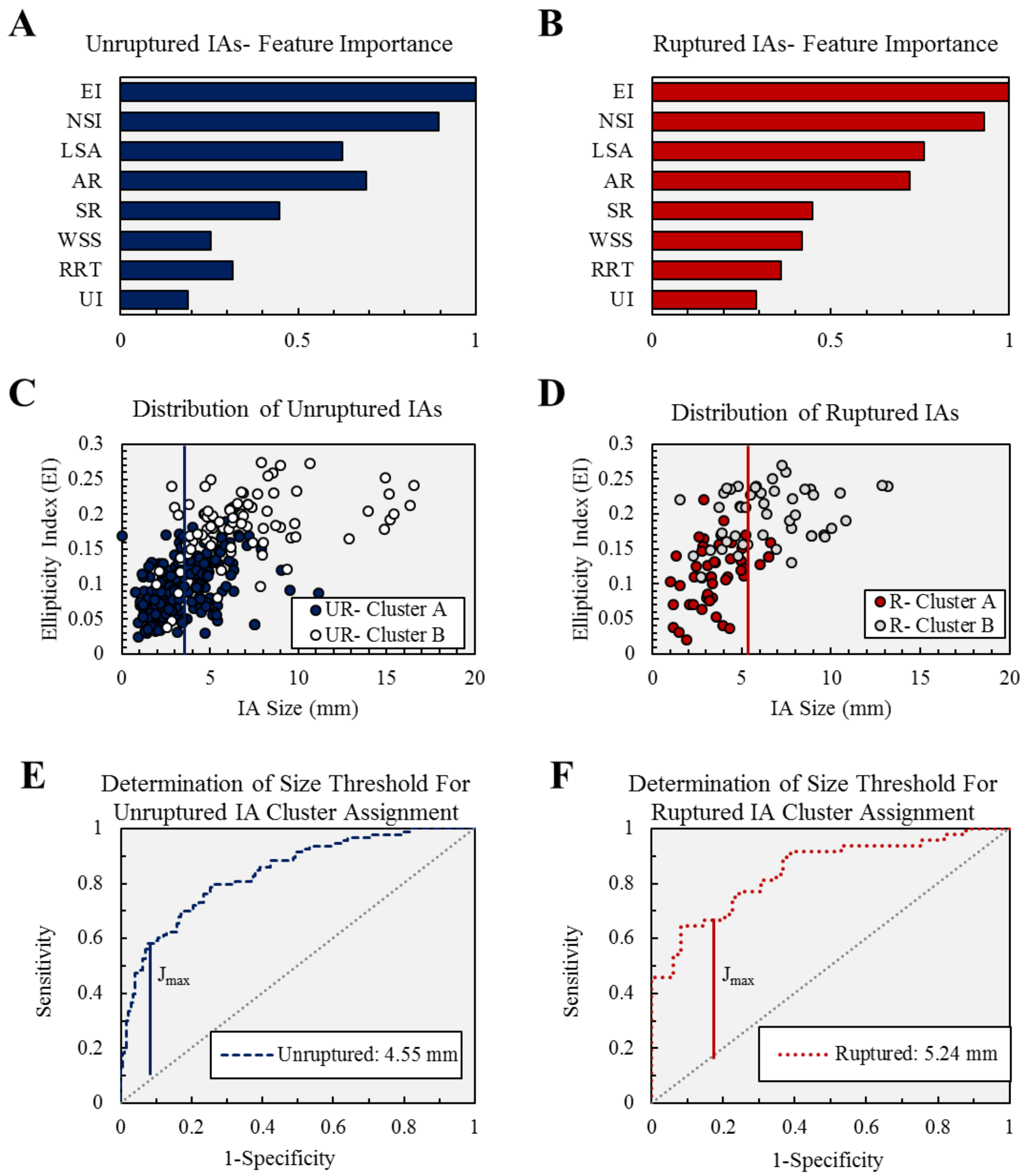

Supplemental Figure I. Determination of the optimal size threshold to separate ruptured and unruptured IAs after hierarchal cluster analysis. The predictor importance for cluster assignment for the (**A**) unruptured and (**B**) ruptured groups. A scatter plot showing EI versus IA size for the (**C**) unruptured and (**D**) ruptured groups indicated that smaller IAs tended to be assigned to Cluster A. Receiver operating characteristic (ROC) curve analysis that showed an optimal size threshold of (**E**) 4.55 mm for the unruptured group and (**F**) 5.24 mm the ruptured group.

AR=aspect ratio, EI=ellipticity index, LSA=low wall shear stress area, NSI=nonsphericity index, RRT=relative residence time; SR=size ratio, UI=undulation index, WSS=wall shear stress.

Supplemental Tables

Supplemental Table I. Morphologic and hemodynamic feature definitions

Abbreviation	Name (Reference)	Definition
Size	Aneurysm size[3, 4]	H_{max}=maximum perpendicular distance of the aneurysm dome to the neck plane
Neck	Neck diameter[4]	D=average neck diameter
SR	Size ratio[4]	$SR = \frac{H_{max}}{D_v}$ D_v=average parent vessel diameter
AR	Aspect Ratio[4]	$AR = \frac{H_{max}}{D}$
UI	Undulation index[3, 4]	$UI = 1 - \frac{V}{V_{ch}}$ V=volume of the aneurysm; V_{ch}=volume of the convex hull
EI	Ellipticity index[3, 4]	$EI = 1 - (18\pi)^{\frac{1}{3}} V_{ch}^{2/3} / S_{ch}$ S_{ch}=surface area of the convex hull
NSI	Nonsphericity index[3, 4]	$NSI = 1 - (18\pi)^{\frac{1}{3}} V^{2/3} / S$ S_{ch}=surface area of the aneurysm
An	Aneurysm number[5]	$An = \frac{W_a}{D_a} PI$ W_a=width of the aneurysm neck; D_a=parent artery diameter; PI=pulsatility index
WSS	Normalized wall shear stress[6]	$WSS = \frac{\frac{1}{T}\int_0^T \lvert WSS_a \rvert dt}{\frac{1}{T}\int_0^T \lvert WSS_V \rvert dt}$ $WSS_{a/V}$=instantaneous shear stress vector for the aneurysm/parent artery; T=cycle period
MWSS	Maximum normalized wall shear stress[6]	$MWSS = max_{A_a}\left(\frac{\frac{1}{T}\int_0^T \lvert WSS_a \rvert dt}{\frac{1}{T}\int_0^T \lvert WSS_V \rvert dt}\right)$ A_a=aneurysmal area
LSA	Low wall shear stress area[6, 15]	$LSA = A_1 / A_a$ A_1=low WSS aneurysm area <10% of parent vessel WSS
WSSG	Wall shear stress gradient[6]	$WSSG = \frac{1}{T}\int_0^T \frac{\partial WSS}{\partial m} dt$ ∂m=flow direction

OSI	Oscillatory shear index[6]	$OSI = \frac{1}{2}\left\{1 - \frac{\left\|\int_0^T WSSdt\right\|}{\int_0^T \|WSS\|dt}\right\}$
RRT	Relative residence time[6]	$RRT = \frac{1}{\frac{1}{T}\left\|\int_0^T WSSdt\right\|}$
EL	Energy loss[8, 16]	$EL = \frac{v_{in}A_{in}\left\{\left(\frac{1}{2}\rho v_{in}^2 + P_{in}\right) - \left(\frac{1}{2}\rho v_{out}^2 + P_{out}\right)\right\}}{V_m}$ $v_{in/out}$=inlet/outlet velocity; $A_{in/out}$=inlet/outlet area; ρ=density; $P_{in/out}$= inlet/outlet pressure; V_m= volume
PLc	Pressure loss coefficient[8, 16]	$PLc = \frac{\left(\frac{1}{2}\rho v_{in}^2 + P_{in}\right) - \left(\frac{1}{2}\rho v_{out}^2 + P_{out}\right)}{\frac{1}{2}\rho v_{in}^2}$

An=aneurysm number; AR=aspect ratio; EI=ellipticity index; EL= energy loss; LSA=low wall shear stress area; MWSS= maximum wall shear stress; NSI=nonsphericity index; OSI=oscillatory shear index; PLc= pressure loss coefficient; RRT= relative residence time; SR=size ratio; UI=undulation index; WSS=wall shear stress; WSSG= wall shear stress gradient

Supplemental Table II. Comparison of small and large intracranial aneurysms (IAs)

	Small IAs (<5mm)		**Large IAs (≥5mm)**		
	Mean±SD	*Range*	*Mean*±SD	*Range*	**p-value**
Morphologic Features					
IA size (mm)	3.15±1.12	0.74–4.99	7.95±3.64	5.01–28.65	<0.001
Neck diameter (mm)	3.84±3.84	0–10.10	5.18±2.04	2.23–16.92	<0.001
SR	1.51±0.82	0.26–4.80	3.33±2.14	0.92–20.13	<0.001
AR	0.92±0.34	0.03–2.21	1.65±0.71	0.45–5.71	<0.001
UI	0.067±0.062	0.006–0.282	0.081±0.063	0.008–0.245	0.030
EI	0.11±0.050	0.02–0.25	0.18±0.05	0.04–0.27	<0.001
NSI	0.13±0.061	0.02–0.32	0.20±0.07	0.04–0.35	<0.001
An	0.94±0.56	0.21–3.45	1.10±0.53	0.300–3.10	<0.001
Hemodynamic Features					
WSS	0.66±0.47	0.03–1.85	0.44±0.32	0.02–1.20	<0.001
OSI	0.007±0.019	0–0.031	0.013±0.044	0–0.120	<0.001
WSSG	-44±198	-1121–1134	-61±297	-3470–138	0.303
RRT	3.02±4.47	0–40.46	5.23±6.84	0.74–47.93	<0.001
LSA	0.14±0.24	0–1	0.27±0.29	0–0.96	<0.001
MWSS	4.03±2.36	0–15.20	4.57±3.57	0.39–32.40	0.171
PLc	4.39±4.21	0–173.06	3.91±4.44	0.19–55.93	0.066
EL (W/m^3)	6178±15034	0–203478	11275±23460	0–120609	<0.001

An=aneurysm number; AR=aspect ratio; EI=ellipticity index; EL= energy loss; LSA=low wall shear stress area; MWSS= maximum wall shear stress; NSI=nonsphericity index; OSI=oscillatory shear index; PLc= pressure loss coefficient; RRT= relative residence time; SD=standard deviation; SR=size ratio; UI=undulation index; WSS=wall shear stress; WSSG= wall shear stress gradient

Supplemental Table III. Comparison of ruptured and unruptured morphologic and hemodynamic features in the aggregate IA group.

	Aggregate		
	Unruptured (n=311) *Mean±SD*	**Ruptured** (n=102) *Mean±SD*	**p-value**
Patient Characteristic			
Age(yrs)	60±12	58±14	0.090
Morphologic Features			
Size(mm)	4.87±3.54	5.12±2.58	0.155
Neck(mm)	4.29±1.87	3.97±1.46	0.238
SR	1.96±1.69	2.81±1.53	<0.001
AR	1.15±0.64	1.33±0.55	0.003
UI	0.062±0.058	0.100±0.07	<0.001
EI	0.12±0.059	0.16±0.058	<0.001
NSI	0.15±0.067	0.19±0.072	<0.001
An	0.91±0.50	1.25±0.61	<0.001
Hemodynamic Features			
WSS	0.60±0.38	0.45±0.38	<0.001
OSI	0.010±0.008	0.020±0.032	<0.001
WSSG	-44±157	-28±177	0.740
RRT	3.00±3.93	5.98±7.82	<0.001
LSA	0.14±0.22	0.32±0.32	<0.001
MWSS	4.24±2.71	3.91±3.02	0.030
PLc	4.37±5.09	16.65±102.30	0.431
EL(W/m^3)	6528±10971	15775±34238	0.042

An=aneurysm number; AR=aspect ratio; EI=ellipticity index; EL= energy loss; LSA=low wall shear stress area; MWSS= maximum wall shear stress; NSI=nonsphericity index; OSI=oscillatory shear index; PLc= pressure loss coefficient; RRT= relative residence time; SD=standard deviation; SR=size ratio; UI=undulation index; WSS=wall shear stress; WSSG= wall shear stress gradient

Supplemental Table IV. Comparison of unruptured and ruptured clinical features in the aggregate IA group.

	Aggregate		
	Unruptured (n=311) *Total(%)*	**Ruptured** (n=102) *Total(%)*	**p-value**
Patient Characteristics			
Female Sex	242(78%)	67(66%)	0.018
Hypertension	170(55%)	57(56%)	0.909
Smoking	156(50%)	42(42%)	0.138
Family hx of IA	39(13%)	12(12%)	1.000
Previous SAH	21(7%)	19(19%)	0.001
CAD	31(10%)	12(12%)	0.581
Dyslipidemia	77(25%)	21(21%)	0.424
Diabetes	27(9%)	13(13%)	0.249
Cocaine	4(1%)	5(5%)	0.045
PKD	6(2%)	3(3%)	0.696
Multiple IAs	104(33%)	18(18%)	0.003
Aneurysm Characteristics			
Location			
ACA	46(15%)	42(41%)	<0.001
ICA	162(52%)	24(24%)	<0.001
MCA	41(13%)	10(10%)	0.488
PCOM	15(5%)	15(15%)	0.002
Posterior	47(15%)	11(11%)	0.326

ACA=anterior cerebral artery; CAD=coronary heart disease; hx=history; ICA=internal carotid artery; MCA=middle cerebral artery; PCOM=posterior communicating artery; PKD=polycystic kidney disease; SAH=subarachnoid hemorrhage; Posterior=posterior circulation (including vertebral, posterior inferior cerebellar, posterior cerebral, superior cerebellar, anterior inferior cerebellar, and basilar artery aneurysms)

Supplemental Table V. Odds ratios and 95% CI for model parameters in the small IA, large IA and aggregate models

Model Parameter	Small IAs	Large IAs	Aggregate
		OR (95% CI)	
UI	1.47(1.20-1.79)	1.46(1.18-1.80)	1.45(1.25-1.69)
OSI	2.63(1.72-4.00)	N/A	4.34(1.90-9.91)
Low WSS	N/A	1.41(1.10-1.80)	1.28(0.95-1.34)
Previous SAH	3.86(1.29-11.51)	7.65(1.28-45.69)	9.55(3.61-25.23)
ACA Location	N/A	7.22(2.03-25.71)	4.07(2.01-8.23)
PCOM Location	N/A	5.77(1.67-19.87)	4.22(1.64-10.89)
Absence of Multiple IAs	2.96(1.13-7.75)	N/A	2.21(1.07-4.55)

ACA=anterior cerebral artery; CI=confidence interval; IA=intracranial aneurysm; N/A=not applicable; OR=odds ratio; OSI=oscillatory shear index; PCOM=posterior communicating artery; SAH=subarrachnoid hemmorage; UI=undulation index; WSS=wall shear stress

Supplemental Table VI. Comparison of oscillatory shear index (OSI) in cases with Jet Breakdown Mode vs. Continuous Jet Mode.*

	Jet Breakdown Mode	**Continuous Jet Mode**	**p-value**
OSI (x10^{-2})	*Mean±SD*	*Mean±SD*	
Small IAs	1.36±2.95	0.62±1.59	0.019
Large IAs	1.55±2.38	0.64±0.91	0.010

*OSI was significantly higher in IA cases with jet breakdown mode.

Supplemental References

1. Antiga L, Piccinelli M, Botti L, Ene-Iordache B, Remuzzi A, Steinman DA. An image-based modeling framework for patient-specific computational hemodynamics. *Med Biol Eng Comput.* 2008;46:1097-1112.

2. Antiga L, Steinman DA. Robust and objective decomposition and mapping of bifurcating vessels. *IEEE Trans Med Imaging.* 2004;23:704-713.

3. Raghavan ML, Ma B, Harbaugh RE. Quantified aneurysm shape and rupture risk. *J Neurosurg.* 2005;102:355-362.

4. Dhar S, Tremmel M, Mocco J, Kim M, Yamamoto J, Siddiqui AH, et al. Morphology parameters for intracranial aneurysm rupture risk assessment. *Neurosurgery.* 2008;63:185-196; discussion 196-187.

5. Le TB, Borazjani I, Sotiropoulos F. Pulsatile flow effects on the hemodynamics of intracranial aneurysms. *J Biomech Eng.* 2010;132:111009.

6. Xiang J, Natarajan SK, Tremmel M, Ma D, Mocco J, Hopkins LN, et al. Hemodynamic-morphologic discriminants for intracranial aneurysm rupture. *Stroke.* 2011;42:144-152.

7. Oka S, Nakai M. Optimality principle in vascular bifurcation. *Biorheology.* 1987;24:737-751.

8. Takao H, Murayama Y, Otsuka S, Qian Y, Mohamed A, Masuda S, et al. Hemodynamic differences between unruptured and ruptured intracranial aneurysms during observation. *Stroke.* 2012;43:1436-1439.

9. Greving JP, Wermer MJ, Brown RD, Jr., Morita A, Juvela S, Yonekura M, et al. Development of the PHASES score for prediction of risk of rupture of intracranial aneurysms: a pooled analysis of six prospective cohort studies. *Lancet Neurol.* 2014;13:59-66.

10. Wiebers DO. Unruptured intracranial aneurysms: natural history, clinical outcome, and risks of surgical and endovascular treatment. *Lancet.* 2003;362:103-110.

11. Crompton MR. Mechanism of growth and rupture in cerebral berry aneurysms. *Br Med J.* 1966;1:1138-1142.

12. Schneiders JJ, Marquering HA, van Ooij P, van den Berg R, Nederveen AJ, Verbaan D, et al. Additional value of intra-aneurysmal hemodynamics in discriminating ruptured versus unruptured intracranial aneurysms. *AJNR Am J Neuroradiol.* 2015;36:1920-1926.

13. Xiang J, Yu J, Choi H, Dolan Fox JM, Snyder KV, Levy EI, et al. Rupture Resemblance Score (RRS): toward risk stratification of unruptured intracranial aneurysms using hemodynamic-morphological discriminants. *J Neurointerv Surg.* 2014.

14. Kashiwazaki D, Kuroda S. Size ratio can highly predict rupture risk in intracranial small (<5 mm) aneurysms. *Stroke.* 2013;44:2169-2173.

15. Jou LD, Lee DH, Morsi H, Mawad ME. Wall shear stress on ruptured and unruptured intracranial aneurysms at the internal carotid artery. *AJNR Am J Neuroradiol.* 2008;29:1761-1767.

16. Qian Y, Takao H, Umezu M, Murayama Y. Risk analysis of unruptured aneurysms using computational fluid dynamics technology: preliminary results. *AJNR Am J Neuroradiol.* 2011;32:1948-1955.